Available online at www.sciencedirect.com

ScienceDirect

Energy Procedia 6 (2011) 413–421

Energy Procedia

MEDGREEN 2011-LB

Simulation of the opti-physical parameters of selectives surfaces of absorber by the FDTD method. « applied to solar water heater »

F.HADDAD[a], A. CHIKOUCHE[b] and M. LAOUR[c]

[a,b,c] Unit Development Solar Equipment *(U.D.E.S)*

U.D.E.S, Route Nationale N° 11, BP 386,Bouismail 42415, W. de TIPAZA, ALGERIE

Abstract

Solar collectors are used for domestic water heating. They are used to collect and convert solar radiation into heat energy, by heating liquid water. One of the most important components of the solar collector is the absorber, which has to have selectivity in the wavelengths of the solar spectrum. This selectivity allows it to have a maximum of absorbance with a minimum of thermal radiation emitted .The objective of our work consists in characterizing these selective surfaces. A selective surface usually consists of a layer or a thin absorbing film in the solar and transparent spectrum in thermal infrared on a metallic support of a weak emission (substratum). We are interested in our work by the simulation of the opti-physical parameters of these selective surfaces using the FDTD method.

The multi-scales(multi-ladders approach), led in this work, will first of all consists in studying the interactions between the electromagnetic waves and the microstructures whose characteristic scales will be close to the wavelength (microphone-scales).The directional and spectral selectivity caused by the microphone-structured surfaces will be modelled finely by solving the Maxwell's equations. The resolution of the Maxwell's equations will be undertaken using the F D T D method.

Keywords: Photo-thermal conversion, solar water heater absorber, spectral selectivity, the FDTD method, optical properties emission, light- material interactions.

Nomenclature

H : incident power (W/m²)	e: Electric field (V/m)
T : temperature (K)	h: Magnetic field (A/m)
P : power lost (W/m²)	ε_r : dielectric constant
α, α` : absorption coefficients	A: Absorbance
ε : coefficient of thermal emissivity	T: Transmittance
η : Performance	μ: Magnetic Permeability

* Corresponding author. Tel.: +213 556728781.

E-mail address: faouzi72dz@yahoo.fr.

doi:10.1016/j.egypro.2011.05.048

1.Introduction

UDES (Development Unit solar equipment) developed in the 1990 the first solar water heater with the absorber that consists of an aluminum plate on which is applied a layer of black paint. The aim of our work is to optimize this layer on the optical, physical and mechanical support perspective. For this, we introduced other types of selective ultrathin layers on two types of media in this case aluminum and copper. There are also other applications that use electromagnetic radiation interactions with matter: solar cells, smart windows, Infrared detectors, satellite communication ... etc. Despite their diversity, all these applications rely on ultra-thin layers on their surfaces whose physical and optical characteristics depend on the wavelengths of the electromagnetic radiation spectrum. Such thin layers deposited on the surfaces act as filters where some photons at wavelengths of data must be able to be reflected or absorbed, while others, at different wavelengths, must be pushed or trapped . This ability to "filter" is a feature of so-called "selective surfaces.

2. Radiative balance and heat balance of an absorber

An absorber, with its rear faces and side perfectly isolated, exposed to solar radiation reaches an equilibrium temperature as the received power equals the power lost. The power received per square meter is the sum of two terms [1]:

$$P_r = \alpha H + \alpha' \sigma T_a^4 \tag{1}$$

The power loss is also a function of two components [1]:

$$P_p = \varepsilon \sigma T^4 + P_c \tag{2}$$

The heat balance per unit area is:

$$\varepsilon \sigma T^4 + P_c = \alpha' \sigma T_E^4 + \alpha H \tag{3}$$

For a surface $\alpha = \alpha' = \varepsilon = 1$, eq (3) becomes:

$$H = P_c + \sigma (T^4 - T_E^4) \tag{4}$$

In the case where part of the absorbed power is converted into heat then transmitted to the fluid, we should consider this power φ_u, either:

$$\varphi_u + \varepsilon \sigma T^4 + P_c = \alpha' \sigma T_E^4 + \alpha H \tag{5}$$

Such For H = constant, we define the conversion efficiency as:η

$$\eta = \frac{\varphi_u}{H} = \alpha + \frac{\alpha' \sigma T_E^4}{H} - \frac{\varepsilon \sigma T^4}{H} - \frac{P_C}{H} \tag{6}$$

Examination of the radiation balance :

$$\eta_R = \alpha \left[1 - \frac{\varepsilon}{\alpha} \frac{\sigma \left(T^4 - T_E^4 \right)}{H} \right] \tag{7}$$

By considering eq (7), we can say that:

- The yield η_R is maximum when $T = T_E$, it means, if there is no rise in temperature of the absorber from the outside temperature.

- It is possible to increase the value of output by increasing the ratio α/ε In view Kirchhoff's law [2], we have, for the wavelength λ :

$$\alpha_\lambda = \varepsilon_\lambda = 1 - R_\lambda \quad (8)$$

Parameters α and ε are based on optical properties of the surface temperature T and wavelength [2]. To reduce the value of (α / ε), the surface must have a low coefficient of reflection for the visible (VIS), while for the infrared (IR), Rλ must be high. Hence obtaining a selective surface for these optical properties varies with the wavelength λ of the spectrum.

3. Selectivity

If we represent the optical properties of a selective absorber real Rλ(λ), there is an increase of Rλ factor in the infrared, whichλa diagram (can be more or less abrupt depending on the selective surface considered. Figure 1 gives an example of such variation, obtained in the case of "chrome", which surface has two distinct areas or Rλ is low for .3≤ λ ≤ 2 µm then equal to 0.9 when λ> 10 mµ The transition between the two are made over a spectral range $\Delta\lambda$ from 2 à 10 µm.

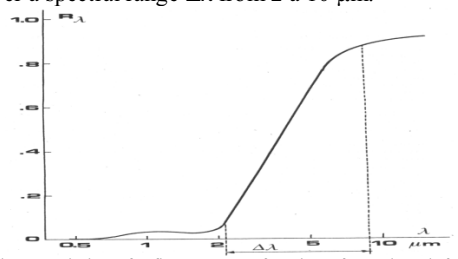

Fig 1. Variation of reflectance as a function of wavelength for a Selective absorber real - for chromium [3]

With regard to the absorptive surface, which can be likened to a "filter high-pass" there is no body in nature, having ideal optical properties required. However, some materials such as chromium, aluminium and copper (Figure 2) have a selective behaviour favourable to the thermal conversion of solar energy.

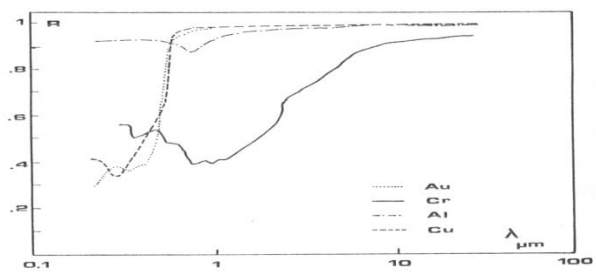

Fig 2. Variation of reflectance as a function of wavelength for Different substrates [3]

4. FDTD Simulations

The light absorbing behavior of solar heater water (SHW) having comprised of TiO2 were examined using Finite Difference Time Domain (FDTD 3D) [7, 8]. In the FDTD analysis, a plan electromagnetic wave is incident onto solar heater water passing through the barrier layer; light that

emerges from (SHW) is reflected by a perfectly electrical conducting layer (PEC) boundary that simulates the effect of solar heater water. An observation plane placed between the electromagnetic source and TiO2 material detects the intensity of both the incident wave and the wave returning back from the SHW structure.

4.1. FDTD Principal

The original FDTD paradigm was described by the Yee cell, [9], named, of course, after Kane Yee Note that the e and h fields are assumed interleaved around a cell whose origin is at the location i, j, k. Every **e** field is located 1/2 cell width from the origin in the direction of its orientation; every **h** field is offset 1/2 cell in each direction except that of its orientation.

Not surprisingly, we will start with Maxwell's equations:

$$\frac{\partial \tilde{d}}{\partial t} = \frac{1}{\sqrt{\varepsilon_0 \cdot \mu_0}} \nabla \times h \tag{9}$$

$$\tilde{d}(\omega) = \varepsilon_r^*(\omega) \cdot \tilde{e}(\omega) \tag{10}$$

$$\frac{\partial h}{\partial t} = -\frac{1}{\sqrt{\varepsilon_0 \cdot \mu_0}} \nabla \times \tilde{e} \tag{11}$$

$$\tilde{e} = \sqrt{\frac{\varepsilon_0}{\mu_0}} \cdot \tilde{e} \tag{12}$$

$$\tilde{d} = \sqrt{\frac{1}{\varepsilon_0 \cdot \mu_0}} \cdot \tilde{d} \tag{13}$$

If we consider component at x direction we have the next expression:

$$\frac{\partial \tilde{d}_x}{\partial t} = \frac{1}{\sqrt{\varepsilon_0 \cdot \mu_0}} \cdot \left(\frac{\partial h_z}{\partial y} - \frac{\partial h_y}{\partial z} \right) \tag{14}$$

$$\frac{\partial h_x}{\partial t} = -\frac{1}{\sqrt{\varepsilon_0 \cdot \mu_0}} \cdot \left(\frac{\partial \tilde{e}_z}{\partial y} - \frac{\partial \tilde{e}_y}{\partial z} \right) \tag{15}$$

So that both space and time have to be discretized. The standard FDTD is based on the Yee algorithm. As we saw in the previous section, central-difference approximations are second-order accurate. To achieve second-order accuracy in time, the Yee algorithm uses a *leapfrog* arrangement. e fields are calculated at $t = n\Delta t$ using previously calculated and stored h fields. Then h fields are calculated at $t = (n+1/2)\Delta t$ using the previously calculated and stored e fields, and the process continues until time-stepping is concluded.

4.2. Treatment of Dispersive Media in FDTD

One of the major challenges in FDTD modeling of metals at optical frequencies is the treatment of the metallic dispersion properties [10, 11]. As mentioned above, in time-domain methods the dielectric constants of dispersive media have to be approximated by suitable analytical expressions. The most

common algorithm for modeling dispersive materials with FDTD is the auxiliary differential equation (ADE) method. In dispersive materials $\varepsilon(\omega)$ relates e and d : $\widetilde{d}(\omega) = \varepsilon_r^*(\omega) \cdot \widetilde{e}(\omega)$.

ADE is based on integrating an ordinary differential equation in time that relates d(t) to e(t), concurrently with Maxwell's equations. This equation is derived by taking the inverse Fourier transform of Eq. (10).

We consider here a simple example where the dielectric constant $\varepsilon_r(\omega)$ consists of a single Lorentzian term.

$$\varepsilon_r(\omega) = \frac{\omega_0^2}{(\omega_0^2 - \omega^2) - i\omega\gamma_0} \tag{16}$$

If we substitute Eq. (15) into Eq. (16) and take the inverse Fourier transform, we obtain a second-order differential equation relating d and e.

Equation (10) is discretized using a second-order accurate central-difference scheme similar to those described above. We note that, if the ADE method is used, e is obtained from h in two steps. First, d is obtained from h by solving the finite-difference approximation of:

$$\nabla \times h = \frac{\partial d}{\partial t} \tag{17}$$

Second, e is obtained from d by solving the finite-difference approximation of Eq. (16). Calculation of the finite-difference expressions of the first and second temporal derivatives of d in Eq. (16) requires storage of 2 previous values of d, in other words not only $d|^{n+1}$ but also $d|^{n}$ and $d|^{n-1}$ are required to obtain e from d.

4.3. FDTD Results of computational Model

The numerical model used in this work is shown in Fig. 3. The TiO2 (SHW) dimensions are defined by the thickness tk=2000nm. While the subtract was represented by a perfect electric conductor (PEC) with 100% light reflection.

The grid size of the FDTD model was set to 2 nm*2 nm*2 nm, the lowest limit based on the 4 GHz processing speed of the computer used for the simulations. The excitation wave, generated at the Source Plane located above the barrier layer of the TiO2 (SHW) array. The excitation source is chosen as a Gaussian electric field.

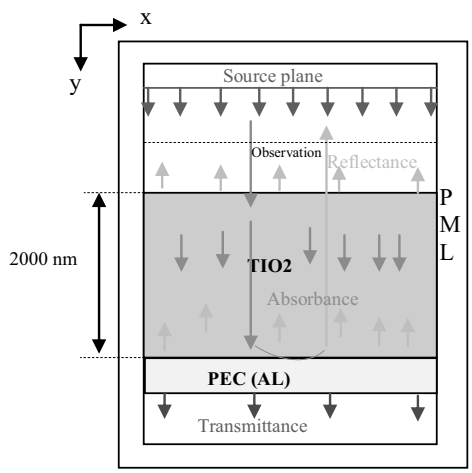

Fig. 3.Tree dimensional FDTD model used for determining the propagation of EM wave through a TiO2(SHW)

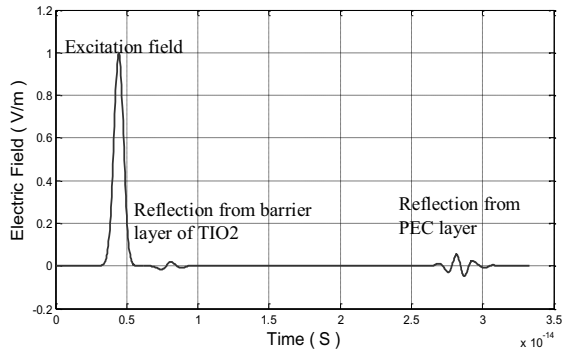

Fig. 4. The observation plane, see Fig. 3 captures the excitation electric field, as well as the electric field reflected from the barrier layer TiO2 (SHW) and reflected from the perfect electrical conductor (PEC) boundary.

Figure 4 shows the electric field captured at the Observation Plane. The excitation center frequency is $3*10^{14}$Hz (wavelength=1000 nm). As shown in the figure, the observation plane captures the excitation field e_i, as well as two packets of fields reflected from the barrier layer TiO2 (SHW) e_1 and from the PEC layer e_2. We ignore the effect of the reflected field e_1 from the barrier layer since it forms only a small part of the excitation field due to the low refractive index TiO2 for a dense film.

The transmitted wave propagates through the barrier layer TiO2 before being reflected from the PEC. This reflected wave travels back through TiO2 and barrier layer and reaches the observation plane carrying information about light-material interactions; this field (e_2) is, hence, referred to as the "transmitted field."

By performing a Fast Fourier Transformation (FFT) on e_i and e_2, as well as the corresponding h_i and h_2, the total incident and "transmitted" field, at fm, is calculated using:

$$p_i = e_i \times h_i^* \tag{18}$$

$$p_t = e_2 \times h_2^* \tag{19}$$

By definition, the transmittance T and absorbance A are calculated from P_i and P_t as:

$$T = {p_t}/{p_i} \times 100\% \tag{20}$$

$$A = 20*\log_{10}\left({p_i}/{p_t} \right) \tag{21}$$

5.Experiments

5.1 Filing of selective layers by dip-coating method

Dip-coating technique is used for deposits made on substrates with translational symmetry. The substrate is immersed in a solution of paint (SOLKOTE HI / SORB II) [7], and is removed from the solution at a constant speed and controlled so that a uniform film covers the submerged surface. This film is left to dry for a few minutes to allow the sol-gel. The withdrawal rate may vary between 1 and 50 cm / min. Dip-coater is used at the UDTS (Development Unit silicon technologies). Figure 5 shows the schematic diagram of the dip-coater that we used.

Fig 5. Photo of Dip-coater

5.2 Fitting experimental measure R (λ)

The experimental curves, R (λ), selective layers deposited by dip-coating technique on various substrates were measured using a spectrophotometer "Spectro 320". This spectrophotometer can scan wavelengths up to 2500 (nm).

5.3 Mounting experimental measure refractive index and thickness

Ellipsometry has been applied in our case to the characterization of materials and deposited layers. Knowing the index of the substrate and that of the deposited layer can then deduct the value of the thickness of the layer. We opted for ellipsometry because of its sensitivity to small variations in thickness.

6. Results and discussions

6.1 Black paint on Aluminum

Initially, we deposited a layer of black paint identical to that applied to our first water heater, manufactured in the 1990s, on an aluminum substrate, after that carried out the characterization by spectroscopy to measure R (λ), Figure 4 shows the reflectance curve as a function of wavelength.

We observe that the black paint produced an increase in absorption coefficient of the absorber plate and the coefficient of thermal emissivity.

6.2 Selective Painting (SOlKOTE HI / SORB II) on Aluminum

In a second step, we chose a second option for selective indication (SOLKOT HI / SORBII). After depositing the various layers from this solution on the aluminum substrate was measured and must be performed to characterize spectroscopically.

The thicknesses of the layers using ellipsometry described above. Figure 6 shows the change in reflectance function λ for different thicknesses of deposited layers B, C, D and E.

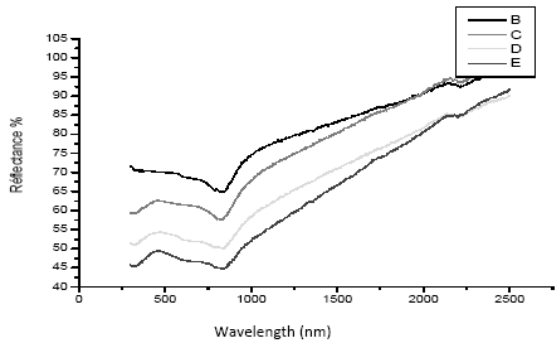

Fig 7. Variation of reflectance as a function of wavelength for different thicknesses

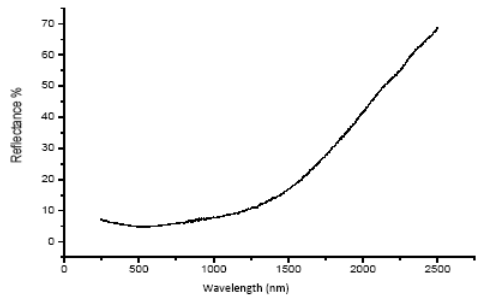

Fig 8**.** Variation of reflectance as a function of wavelength for an optimal thickness of 2.5 µ m [4].

There was a reduction of the reflectance gradually as the thickness of layers increases (curves B, C, D, E). The thicknesses and refractive indices are shown in Table 1.

Table 1. Thicknesses and refractive indices of layers SOLKOTE HI / SORB II.

Layers	B	C	D	E
Thickness (nm)	240	415	565	695
Refractive indices	1 .54	1.58	1.60	1.61

Figure 8 shows the change in reflectance as a function of wavelength for an optimal thickness of 2.5 µ m. which confirms the good selectivity of this solution.

6.3 Deposit of TiO_2 on a copper substrate

Finally, we characterized by spectroscopy of TiO2 layers deposited on copper substrates (case of an absorber of solar water heaters manufactured by Isofoton SA) [5].

The reflectance curve as a function of wavelength is shown in figure 9.

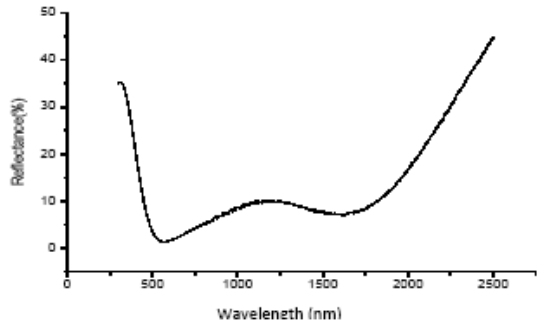

Fig 9. Variation refelectance according to the wavelength
For an optimal thickness 20 µ m TiO2 [5].

There is a good selectivity of the deposited layers for two ranges of the spectrum (VIS) and (IR).

7.*Conclusion*

These results of the deposition of one or more layers selectively allow a significant increase in conversion efficiency of the (ESC). It is in this case we can consider the realization of high performance absorbers. Using these layers, we found an improvement in conversion efficiency of 10 to 17%. Selective layers deposited and characterized helped to highlight the effect of selectivity of the solution SOLKOT HI / SORBII on aluminum and copper on TiO2. The choice of technologies selective deposition of these layers must be simple and economical.

We used FDTD3D to study the propagation of light through layers selectively material for the desired light- material interactions. With FDTD3D, the space containing the object of interest is divided into three-dimensional grids, on the basis of the Maxwell's equations, the FDTD operator updates the electric and magnetic fields in all grids at increasing time steps, allowing determination of the electromagnetic wave in real time. Our efforts demonstrate FDTD to be a broadly applicable technique capable of guiding design of an optimal SHW architecture.

8. *References*

[1]. P.Gallet, F.Papini et G.Péri, "Physique des convertisseurs héliothermiques", EDISUD, 1980.
[2]. J. A. Duffie et W. A. Beckman, "Solar energy of thermal process", Wiley, New York, 1974.
[3]. G. Peri, 'Les capteurs convertisseurs héliothermiques sous concentration'', Association française pour l'étude et le développement de l'énergie solaire, Cahier n°4, Paris 1977.
[4]. www.solec.org, document technique de SOIKOTE HI/SORB II, accessed, 23/12/2010.
[5]. www.isofoton.com , document technique chauffe eau solaire Isofoton plus, accessed, 09/06/2010.
[6]. M. Van Der Leij, "Spectral-selective surfaces for the thermal conversion of solar energy", Thesis Ph.D, Université de Delft, 1979.
[7]. Park J, Bauer S, von der Mark K, Schmuki P (2007) Nanosize and vitality: TiO2 nanotube diameter directs cell fate. Nano Lett 7:1686–1691.
[8]. Craig A. Grimes, Gopal K. Mor « TiO2 Nanotube Arrays Synthesis, Properties, and Applications", Springer Dordrecht Heidelberg London New York, 2009.
[9]. DENNIS M. SULLIVAN, ELETROMAGNETIC SIIMULATION USING THE FDTD METHOD (IEEE Microwave Theory and Techniques Society. New York. 2000).
[10]. A. Vial, A. S. Grimault, D. Macias, D. Barchiesi, and M. L. de la Chapelle, Improved analytical fit of gold dispersion: application to the modeling of extinction spectra with a finite-difference time-domain method, *Phys. Rev. B* **71**(8), 85416 (2005).
[11]. W. L. Barnes, A. Dereux, and T. W. Ebbesen, Surface plasmon subwavelength optics, *Nature* 424, 824-830 (2003).